Measuring Permeability in Acute Ischemic Stroke

Andrea Kassner, PhD[a,*], Daniel M. Mandell, MD, FRCPC[b], David J. Mikulis, MD, FRCPC[b]

KEYWORDS

• MRI • CT • Stroke • Dynamic contrast-enhanced imaging • Hemorrhagic transformation • Permeability

Thrombolytic therapy with recombinant tissue plasminogen activators (rtPA) is the main treatment available for acute ischemic stroke, yet use of rtPA is currently limited to patients presenting within 4.5 hours of symptom onset, because of the increased risk of hemorrhagic transformation (HT) if it is administered later.[1,2] There is strong evidence that the HT process begins at the microvascular level.[3] There are also a growing number of reports implicating rtPA as either a primary cause or as an aggravating factor in BBB breakdown.[4–8] Following intravenous injection of contrast material, extravasation of contrast (through a damaged BBB) is an accurate predictor of subsequent HT. Imaging assessment of BBB integrity may predict the likelihood of hemorrhagic transformation on a patient-by-patient basis, rather than using the same simple 4.5-hour time limit for all patients. This could potentially extend the therapeutic time window in patients with evidence of BBB stability, and potentially exclude some patients from receiving rtPA if they have a high risk of hemorrhage despite falling within the 4.5-hour time window. In this article, we discuss the application of permeability imaging in acute ischemic stroke using MRI and CT.

MRI METHODS FOR THE ASSESSMENT OF BBB INTEGRITY

In the 1980s, the introduction of paramagnetic intravascular contrast agents, such as gadolinium chelate gadopentetate dimeglumine (Gd-DTPA), made possible the investigation of BBB integrity using MRI. Gd-DTPA is the most widely used MR contrast agent. It is a freely diffusible, extracellular tracer with a molecular size of 550 Da. The chelator moiety, DTPA, governs the kinetics of the entire compound and clearance occurs primarily via glomerular filtration. The contrast enhancement is produced by the paramagnetic Gd^{3+} core of the agent, which is known to reduce T1 in a concentration-dependent manner.[9]

For assessment of permeability, Gd-DTPA is administered intravenously, usually as a bolus (manual or power) injection. As the contrast agent passes through the microvasculature of the brain, it is almost entirely confined to the intravascular space. In regions of BBB breakdown, however, the contrast-agent can extravasate and accumulate in the interstitium. Once in the extravascular space, voxels with higher concentrations of contrast agent will appear bright on T1-weighted MR images. We will now discuss the use of

This work was supported by the Canada Research Chair Program and the Canadian Institutes of Health Research.

[a] Department of Medical Imaging, University of Toronto, 150 College Street, Room 125, Toronto, ON M5S 3E2, Canada
[b] Department of Medical Imaging, Toronto Western Hospital, University of Toronto, 399 Bathurst Street, Toronto, ON M5T 2S8, Canada
* Corresponding author.
E-mail address: andrea.kassner@utoronto.ca

Neuroimag Clin N Am 21 (2011) 315–325
doi:10.1016/j.nic.2011.01.004

standard (static) postcontrast T1-weighted MR imaging and dynamic contrast-enhanced MR imaging for the detection of BBB breakdown.

Postcontrast T1-Weighted MRI to Predict HT in Acute Ischemic Stroke

The detection of contrast leakage into brain parenchyma can be attempted with static T1-weighted MR imaging. As with brain tumors, the rationale for static contrast-enhanced MRI is that any tissue supplied by vessels with compromised BBB should eventually become conspicuous as a region of signal enhancement on T1-weighted images. Enhancement on T1-weighted images in hyperacute infarcts is indeed associated with subsequent HT.[10–12] High-resolution T1-weighted images are generally acquired at least several minutes after the intravenous (IV) bolus injection of contrast agent (usually 0.1 mmol/kg Gd-DTPA) to allow for sufficient tracer accumulation in the parenchyma at sites of BBB disruption. Although qualitative visual evidence of parenchymal enhancement (that is, contrast extravasation) on postcontrast T1-weighted MRI is a highly specific (specificity ~85%) predictor of HT, it is infrequent during the crucial hours after symptom onset,[11,13–16] and insensitive (sensitivity ~35%), which may make the test unsuitable for therapeutic decision making.[10–12] Because it provides only a "snapshot" of a dynamic process (ie, contrast extravasation via breaches in BBB integrity), postcontrast T1-weighted MRI could be problematic during the hyperacute or acute phase of injury in acute ischemic stroke. Postcontrast T1-weighted images of 2 HT cases imaged fewer than 6 hours after symptom onset at our institution are provided in **Fig. 1** to illustrate this problem. At present, it remains to be demonstrated that these images can be acquired at just the right moment to capture the onset of BBB breakdown and offer adequate sensitivity within the current 4.5-hour treatment window.

In part, the low sensitivity of postcontrast T1-weighted MRI for secondary hemorrhage may be a consequence of persistent ischemia or microvascular obstruction in the acute phase[17] such that contrast fails to accumulate sufficiently within the infarct despite local BBB disruption. A 1999 report demonstrated that the addition of a continuous low-dose infusion of contrast to the initial bolus dose could improve the sensitivity of postcontrast T1-weighted MRI.[13] Although a lengthy infusion is clearly unsuitable for the purpose of acute ischemic stroke treatment decision making, the development of convenient measures that increase the signal-to-noise ratio (SNR) may enable us to detect BBB disruption, where it exists.

Dynamic Contrast-Enhanced MRI

Rationale and acquisition strategy

Dynamic contrast-enhanced MRI (DCE-MRI) typically involves intravenous bolus injection of a gadolinium contrast agent followed by T1-weighted gradient-recalled echo (GRE) imaging of the brain repeated dozens of times over the course of several minutes. Then, assuming a linear relationship between image MR signal intensity as a function of time ($SI[t]$) and contrast-agent concentration as a function of time ($C[t]$), one can generate a set of concentration versus time curves for each voxel or region of the brain. One also typically generates at least one curve consisting exclusively of blood plasma data ($C[p]$) (**Fig. 2**A). As with postcontrast T1-weighted imaging, evidence of enhancement indicates that contrast material has escaped the confines of the intravascular compartment via breaches in the BBB. The advantage of the dynamic T1-weighted imaging technique is that one can quantify contrast accumulation as a function of time, apply an appropriate pharmacokinetic model to the time-varying $C(t)$ and $C(p)$ data-sets, and estimate BBB permeability in standard units of mL/100 g/min.

The most common MRI sequence used in brain DCE-studies, including those performed at our institution, is a 3-dimensional (3D) GRE sequence with a short repetition-time (TR), short echo-time (TE), and a flip angle of approximately 20° at 1.5 T.[18] Three-dimensional volume acquisitions are favored over 2D equivalents in DCE-MRI of the brain, as they permit the simultaneous sampling of the signal intensity in tissue and in blood and are more likely to encompass a large vessel from which one can generate an arterial input function (a considerable challenge in brain DCE[19]). In addition to coverage, a 3D DCE acquisition offers the advantage of maximizing the saturation of inflowing blood while minimizing precontrast inflow enhancement.[20] Furthermore, the 3D GRE sequence is less sensitive to geometric distortions or magnetic susceptibility than equivalent echo-planar sequences.

The temporal resolution of the DCE sequence must be sufficient to capture the blood-brain flow of contrast anticipated for the pathology of interest. By definition, the temporal resolution of the acquisition will improve with shorter TRs (ie, more images can be collected per unit time); TE should also be short, but this choice is related more directly to mitigating susceptibility-related signal loss caused by the transit of the

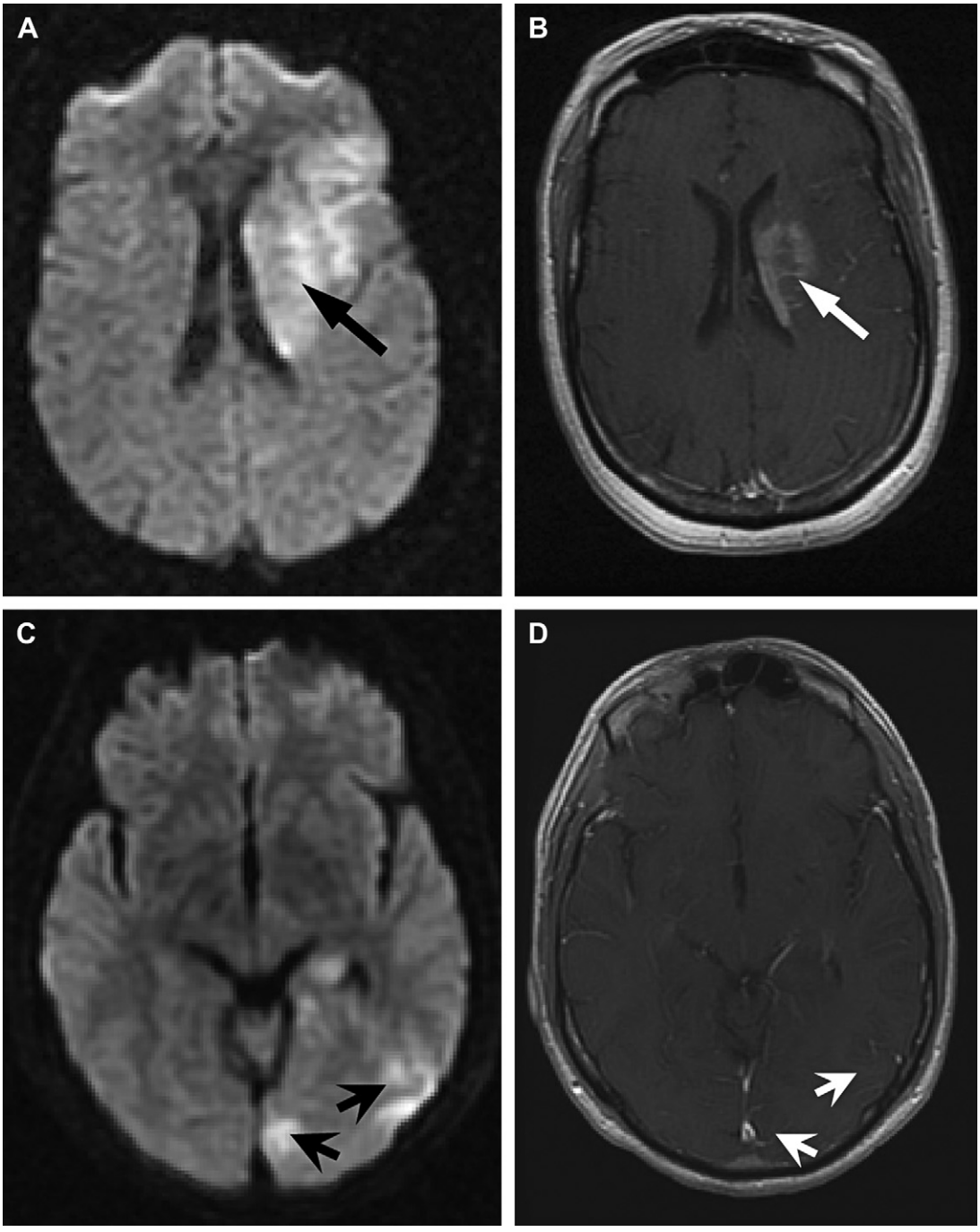

Fig. 1. Diffusion-weighted and postcontrast T1-weighted images for 2 acute ischemic stroke patients who proceeded to hemorrhage. Top: An 81-year-old female patient with acute ischemic stroke, visible as hyperintensity (*arrow*) on the diffusion-weighted image acquired at 3 hours after symptom onset (*A*). The acute ischemic stroke lesion in *A* (*arrow*) corresponds to an area of visible enhancement on the equivalent postcontrast T1-weighted image (*B, arrow*). Bottom: A 69-year-old male patient with acute ischemic stroke, visible as hyperintensity (*arrowhead*) on the diffusion-weighted image acquired at 5 hours 40 minutes after stroke (*C*). Unlike the previous case, the area of ischemia depicted by the diffusion-weighted image did not appear to correspond to any visible gadolinium enhancement in the equivalent T1-weighted image for this patient (*D, arrowhead*).

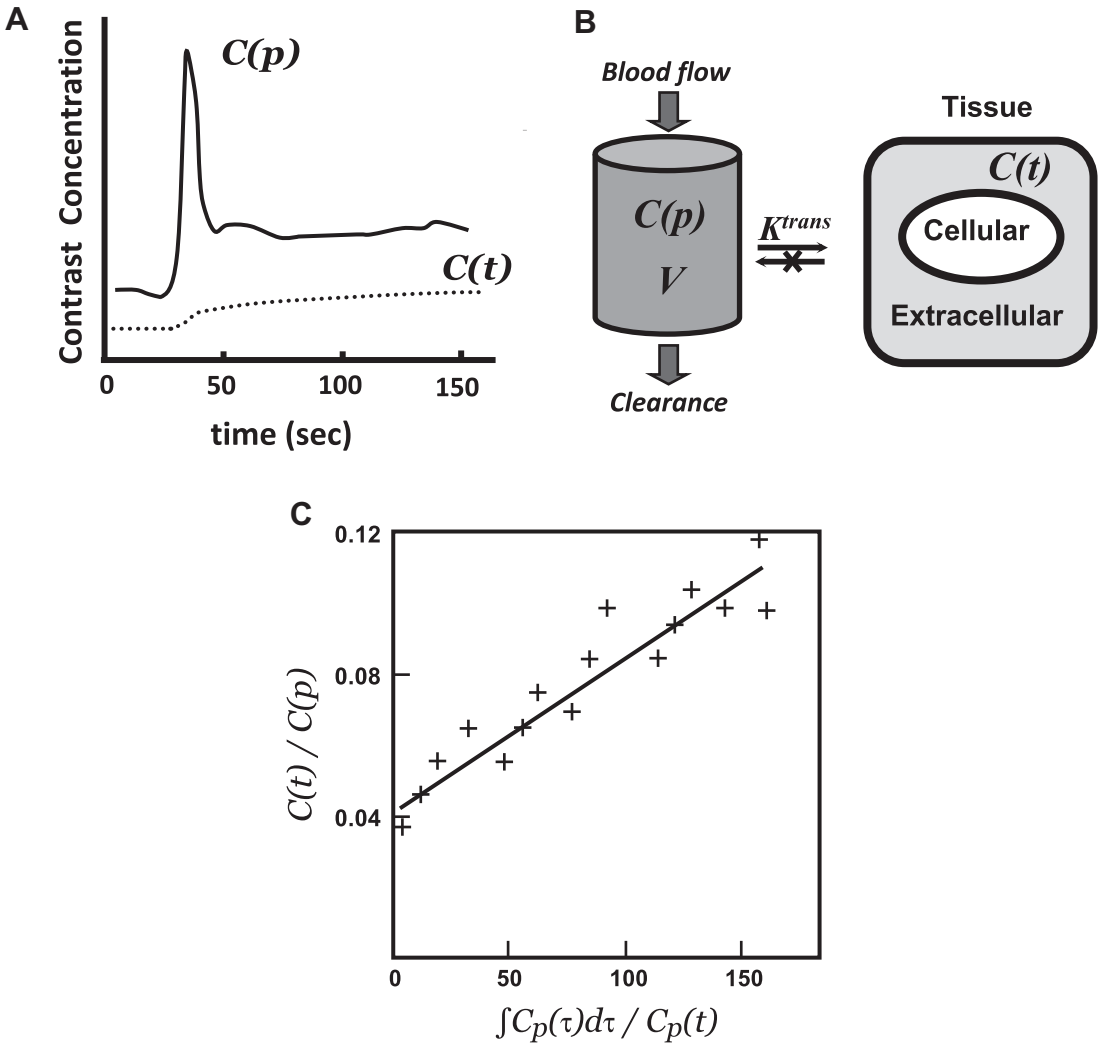

Fig. 2. The contrast concentration versus time curves for both blood plasma (*C[p]*, *solid line*) and tissue (*C[t]*, *dotted line*) are depicted in (*A*). Permeability can be estimated using a unidirectional 2-compartment tracer-kinetic model (*B*), such as the Patlak model.[27] Plotting the ratio $C(t)/C(p)$ versus $\int C_p(\tau)d\tau/C_p(t)$ yields a linear relationship, where permeability (*KPS*) is the slope of best fit (*C*).

paramagnetic contrast-agent through the microvasculature.[21] The TR prescribed for brain DCE-MRI studies is typically less than 10 ms. Although a 3D volume acquisition necessarily increases TR relative to single-slice approaches, this is becoming less of an issue as more centers gain access to parallel imaging techniques (eg, sensitivity encoding using multiple receiver coils[22]).

Pharmacokinetic modeling The initial step in pharmacokinetic analysis is the conversion of MR signal intensity to contrast-agent concentration. The difference in SI between pre- and postcontrast images using a T1-weighted GRE sequence can be expressed as:

$$\triangle SI = k\left(\frac{1}{T_{1post}} - \frac{1}{T_{1pre}}\right)$$

$$= k \triangle \left(\frac{1}{T_1}\right) = k \triangle R_1 \quad (1)$$

where k is a proportionality constant, and R_1 is the longitudinal relaxation rate expressed as 1/T1. One has transitioned from ΔSI to ΔR_1, and after that, one needs to determine the relationship between ΔR_1 and $C(t)$. It is assumed that ΔR_1 is related to $C(t)$ by a linear scaling factor, r_1 (ie, T_1

relaxivity, in s^{-1} mM^{-1}). Given that local tissue environments can modulate tracer relaxivity, this simplification may introduce errors in the final parameter estimates.[23]

The next step is to model the relationship of the tissue contrast agent concentration *C(t)* to the concentration time curve of the contrast agent in blood *C(p)* to gain insight into the physiological process of exchange of the agent between the intravascular and the extracellular space. To achieve this, concentration time curves from both tissue of interest and reference vascular structures are mathematically fitted using a pharmacokinetic model, which enables the derivation of quantitative modeling parameters.

In many cases, the pharmacokinetic models that are applied to DCE-MRI data were originally developed for nuclear medicine tracers.[24–28] Most of these are compartmental models, which define the tissue space as a volume with both intravascular and extravascular compartments. The generalized 2-compartment analysis proposed by Tofts and colleagues[29] defines 2 tracer parameters of physiological interest: the transfer constant, K^{trans} [s^{-1}] and the distribution volume, v_e (ie, the fraction of the extravascular-extracellular space occupied by tracer in mL/g):

$$\frac{dC_t(t)}{dx} = K^{trans}\left[C_p(t) - \left(\frac{C_t(t)}{v_e}\right)\right] \quad (2)$$

When the concentration of contrast in the tissue before injection is 0, that is $C(t)_0 = 0$, we can find a solution to Equation (2) and therefore determine the *C(t)* for each time point postinjection:

$$C_t(t) = K^{trans}\int_0^t C_p(\tau)e^{-\frac{K^{trans}}{v_e}\cdot(t-\tau)} \quad (3)$$

$$d\tau = K^{trans}C_p(t)\otimes e^{-\frac{K^{trans}}{v_e}\cdot t} \quad (4)$$

where $C_t(t)$ is the tissue concentration *C(t)*, $C_p(t)$ is the plasma concentration *C(p)* over time, and the $\otimes$ symbol indicates the convolution operator.

The physiological interpretation of K^{trans} will be specific to the tissue or pathology of interest. Furthermore, K^{trans} will depend on whether the intercompartmental movement of tracer is restricted primarily by capillary permeability or, rather, movement is limited by regional blood flow (*F*, in mL/min/g), ie, $K^{trans} = EF\rho\ (1 - rHct)$, where *E* represents the fraction of contrast agent that extravasates during the first circuit through the vasculature (extraction fraction), ρ indicates the density of the tissue in g/mL, and *Hct* is the hematocrit (the fraction of blood-volume occupied by cells). In addition to flow, *E* is also related to the permeability surface-area product (*PS* in mL/min/g), $E = 1 - exp(-PS/F)$. Taken together, we can see that K^{trans} will predominantly reflect regional blood flow when *PS*/*F* is high ($K^{trans} \sim F\rho\ [1 - Hct]$). Conversely, if *PS*/*F* <1, as is typically the case for clinical MRI contrast media in normal brain parenchyma (and intact BBB), then K^{trans} will be equivalent to $PS\rho$.[18] (Note: K^{trans} is sometimes referred to as *KPS* under these conditions.)

If we consider the permeability-limited scenario and we further assume that there is no efflux of contrast, ie, the tracer becomes effectively "trapped" in the extravascular compartment, at least for the time-scale involved in the tracer-kinetic study, then we can simplify the pharmacokinetic model in the manner proposed by Patlak and colleagues[27] and depicted in **Fig. 2**B. The Patlak model is a graphical approach for estimating *KPS* that models the relationship between $C_t(t)$ and $C_p(t)$ (the input function) using linear regression:

$$\frac{C_t(t)}{C_p(t)} = KPS\cdot\int_0^t \frac{C_p(\tau)d\tau}{C_p(t)} + V \quad (5)$$

where *V* represents the fractional blood volume in each voxel. Plotting the ratio $C_t(t)/C_p(t)$ versus $\int C_p(\tau)d\tau/C_p$ yields a linear relationship, where *KPS* is the slope of best fit and *V* is the y-intercept (see **Fig. 2**C). This approach obviates the need for deconvolution (and its sensitivity to noise). The Patlak model has been adapted and successfully applied to DCE-MRI data obtained in both brain tumors[30] and acute ischemic stroke[20,31] for the estimation of *KPS*.

DCE-MRI for the prediction of HT in acute ischemic stroke

DCE-MRI may aid in selecting acute ischemic stroke patients for treatment based on imaging evidence of BBB integrity (that is, lack of BBB disruption). Using DCE-MRI in an ischemic stroke rat model, Knight and colleagues[32] found that progressive parenchymal enhancement was highly correlated with the presence of HT after reperfusion. After observing elevations in BBB permeability with DCE-MRI, even in the absence of visible postcontrast T1-weighted enhancement in patients who have subsequently hemorrhaged (**Fig. 3**), we added a DCE-MRI component to our acute ischemic stroke MRI protocol. A pilot study of 10 patients with acute ischemic stroke assessed within 24 hours of symptom onset (and not treated with rtPA) showed that it was feasible to measure *KPS* in a clinical acute ischemic stroke setting.[20] Follow-up imaging indicated that 3 of these patients converted to hemorrhage within 48 hours,

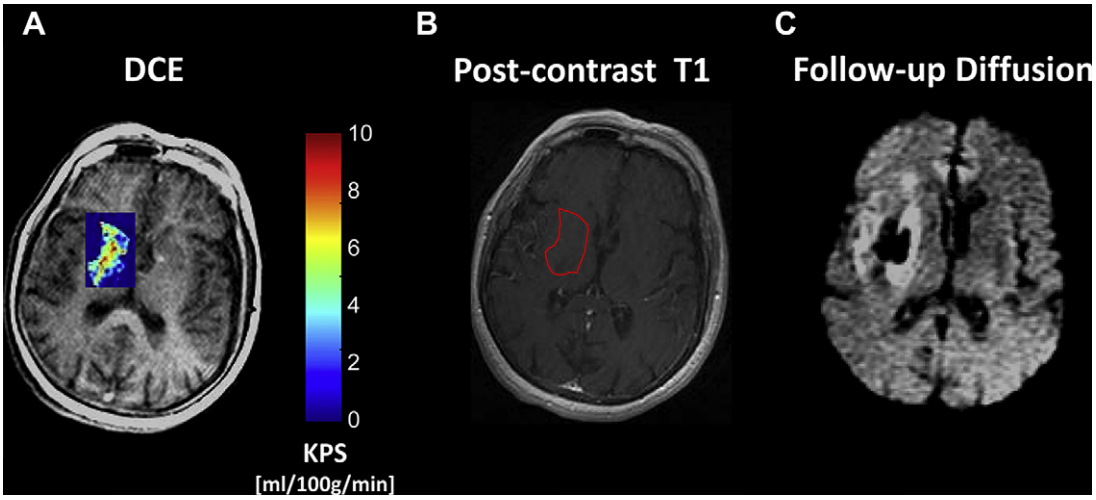

Fig. 3. *KPS* map superimposed on the equivalent DCE image obtained from a 73-year-old patient with acute ischemic stroke who subsequently hemorrhaged (*A*). There was no visible evidence of gadolinium enhancement on the equivalent static postcontrast T1-weighted image (*B*). Both (*A*) and (*B*) were acquired approximately 3 hours following stroke onset. Diffusion-weighted MR imaging performed 48 hours later (*C*) revealed a region of very low signal intensity within a region of hyperintensity, characteristic of hemorrhagic transformation.

and a retrospective analysis found significantly elevated *KPS* in infarcts that progressed to hemorrhage, compared with those in the non-HT group (*KPS* = 3.10 ± 0.44 mL/100 g/min in the HT group vs *KPS* = 0.12 ± 0.10 mL/100 g/min in the non-HT group; $P<.02$).[20] Intrigued by these results, we decided to perform a larger examination of DCE-MRI in acute ischemic stroke, comparing patients who received rtPA with untreated patients who presented to the emergency department within 4 hours of symptom onset.[33] Nine of the 33 patients with acute ischemic stroke who were studied showed progressive enhancement associated with increased permeability in the acute phase (5 received rtPA, 4 were untreated), all of whom proceeded to HT at 48 hours after symptom onset. The mean *KPS* in the HT infarcts was significantly elevated relative to the contralateral hemisphere (within-subjects), and significantly greater than in non-HT infarcts (between-subjects). This was observed in all HT cases, regardless of whether or not the subject received rtPA. With enough data, we may be able to derive a "permeability threshold," or *KPS* value capable of delineating between "low" and "high" risk of HT. The patients with acute ischemic stroke who would benefit the most from this type of stratification would be those who are otherwise excluded from thrombolytic therapy because they present beyond the current 4.5-hour time window for thrombolysis.

Establishing a single receiver operating characteristic (ROC) threshold for the prediction of HT, however, may be a challenge. Ding and colleagues[34] observed that BBB permeability appears to evolve over the course of the acute phase in their rat model of embolic stroke. The investigators found that at 3 hours after symptom onset, *KPS* measured in infarcts that later hemorrhaged was 44% greater than in those that did not, but this discrepancy rose to 167% by 24 hours. As with static postcontrast T1-weighted enhancement, DCE-MR imaging of BBB permeability may be attempting to image a "moving target." Curiously, and on a smaller time scale, a trend toward *decreasing KPS* estimates within the same scan has been observed in patients with acute ischemic stroke, with the *KPS* of HT infarcts exceeding 12 mL/100 g/min when the first 2.5 minutes of DCE-MRI data were used to calculate the estimate, and diminishing to approximately 3.5 mL/100 g/min when the full 4.8 minutes of data were used to approximate permeability in the same infarcts.[35] A similar phenomenon has been reported in the CT permeability imaging literature, whereby permeability values derived from first-pass data increased (3 minutes postcontrast) estimates by approximately fivefold in patients with acute ischemic stroke (7.6 vs 1.3 mL/100 g/min in infarcts).[36] We do not believe, however, that the decline in *KPS* reflects a true decrease in microvascular permeability during the course of DCE-MRI acquisition. Rather, accurate approximations of true microvascular permeability are more likely when the transfer of contrast between the blood and tissue compartments is "close" to equilibrium. To respect the assumptions inherent in the Patlak model, the tracer concentration versus time data must be acquired after

blood-tissue equilibrium has been attained, that is, when the transfer of contrast between compartments is no longer dominated by the rapid changes associated with contrast wash-in.[27] Deviation from this assumption results in nonlinearity of the Patlak plot, perhaps manifesting in a steep rise followed by a rapid recession in C_t/C_p. Although it is still possible to perform linear regression, it is unlikely that the slope of best-fit would reflect true *KPS* in this scenario.

CT METHODS FOR THE ASSESSMENT OF BBB INTEGRITY

CT offers an alternative to MRI for mapping permeability in patients with acute ischemic stroke. Whereas DCE-MRI involves intravenous injection of a paramagnetic contrast agent and voxel-wise measurement of MR signal intensity as a function of time, dynamic contrast-enhanced CT involves intravenous injection of an iodinated contrast agent and voxel-wise measurement of attenuation coefficient (Hounsfield units) as a function of time. The subsequent pharmacokinetic modeling is similar for DCE-CT and DCE-MRI, as discussed previously. **Fig. 4** is an example of a CT permeability map obtained in an acute stroke patient. The image shows a region of increased permeability, with subsequent corresponding hemorrhagic transformation.

Advantages of the CT technique over MRI mainly pertain to availability, accessibility, and speed of CT in the acute stroke setting. These advantages are particularly realized at institutes already performing nonenhanced CT followed by CT angiography (CTA) and/or CT perfusion (CTP) for acute stroke. A major limitation of CTP has been limited craniocaudal spatial coverage, but this will not be an issue with the next generation of multidetector CT scanners.

In 2007, Lin and colleagues[37] reported the use of standard CTP data to map permeability. This group retrospectively reanalyzed first-pass dynamic CTP data (60-second cine acquisition) from 50 patients imaged within 3 hours of onset of acute ischemic stroke, and used the Patlak model to generate maps of permeability. In total, 6 of 50 patients had hemorrhagic transformation. Permeability surface area product (PS) ranged from 5.2 to 13.0 (mean: 9.8 $\pm$ 2.9) in infarcts with hemorrhage transformation, versus 0 to 5.9 (mean: 2.7 $\pm$ 2.0; $P<.0001$) in infarcts without hemorrhagic transformation. A PS threshold of 5.16 mL/100 mL/min yielded a sensitivity and specificity of 100% and 88.7% for prediction of hemorrhagic transformation, and the mean area under the ROC curve was 0.981. A limitation of this study was that the Patlak model was applied to first-pass data, but this model was intended for use only after a steady-state phase of contrast

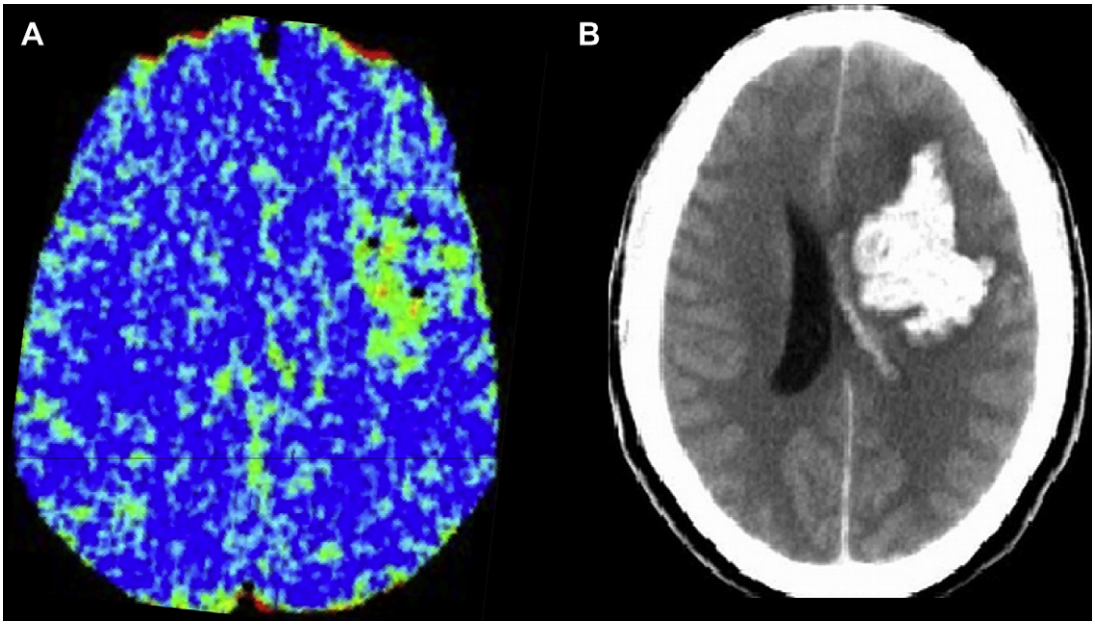

Fig. 4. Map of brain permeability (*A*) obtained using DCE-CT, in a patient with a left MCA territory acute ischemic stroke, demonstrates a large region of increased permeability (*green*) in the left MCA territory. A nonenhanced CT study performed 10 hours later shows hemorrhagic conversion (*B*) in the corresponding region. (Images courtesy of Dr Max Wintermark, Division of Neuroradiology, University of Virginia.)

transfer between the intravascular and extravascular compartments.

Dankbaar and colleagues[36] demonstrated empirically that, indeed, use of first-pass CTP data results in incorrect permeability values, and generates delayed perfusion information rather than permeability. Specifically, Dankbaar and colleagues found that first-pass CTP data yield an overestimation of permeability. Subsequently, Hom and colleagues[38] performed a study to determine how long a delay in acquisition is needed to achieve steady state, and generate accurate permeability values. They found that the CTP acquisition should extend for at least 210 seconds. A longer delay must be balanced against the increased likelihood of head motion with a longer acquisition, and potentially increased radiation dose as well.

Recognizing the need for a longer CTP acquisition, Aviv and colleagues[39] performed a prospective study using a 2-phase CTP acquisition to determine whether PS values distinguish patients with acute stroke who are likely to develop hemorrhagic transformation from those who are not. They reported on 41 patients with acute ischemic stroke who underwent imaging within 3 hours of symptom onset. A CTA was performed from the aortic arch through the vertex, followed by a second bolus of contrast injection, a 45-second continuous CTP acquisition, and then a 90-second CTP acquisition with an image acquired every 15 seconds. In this study, 23 of 41 patients developed hemorrhagic transformation. A PS threshold of 0.23 mL/100 mL/min yielded a sensitivity and specificity of 77% and 94% for prediction of hemorrhagic transformation, and the mean area under the ROC curve was 0.918. One question arising from this study was whether residual contrast material from the CTA affects the accuracy of the subsequent permeability measurement. Does saturation of the parenchymal compartment from the first bolus decrease the amount of contrast extravasation following the second bolus?[36] This theoretical possibility might require further investigation.

SUMMARY AND FUTURE DIRECTIONS FOR IMAGING ASSESSMENT OF BBB INTEGRITY

The term "permeability imaging" is currently used for MR and CT techniques to map disruption of the BBB. In the context of MRI, it involves either a qualitative (static postcontrast T1-weighted imaging) or quantitative (typically, DCE) technique. In the context of CT, it involves either standard or extended CTP acquisitions. Qualitative evidence of parenchymal contrast enhancement on T1-weighted static MRI is a specific, but not sensitive indicator of BBB disruption. Furthermore, visual assessment of gadolinium enhancement is unsuitable for the longitudinal study of permeability desired for clinical trials. There is a recognized need to identify incremental changes in microvascular permeability to evaluate the effectiveness of rtPA for acute ischemic stroke. In contradistinction, DCE-MRI may indeed provide a robust tool for assessing the effects of such therapies on HT, but more guidance is required regarding the appropriate selection of MR end points. Although we have endeavored to emphasize the relative strengths and weaknesses of both CT and MRI approaches, the choice of technique will also depend on institutional expertise. This is particularly true of the dynamic techniques, as they require familiarity with pharmacokinetic modeling or at least the interpretation of the parameter estimates provided by the software.

Several investigators have proposed MRI alternatives to T1-based DCE MRI, aimed to extract permeability-related information from routine clinical perfusion-weighted images.[40–42] Perfusion imaging with dynamic susceptibility contrast (DSC) MRI is a mainstay of most acute ischemic stroke evaluation protocols and can be acquired in less than 2 minutes. Like DCE, DSC imaging involves tracking the passage of an intravenously administered bolus of gadolinium contrast agent with a series of MR images. The high magnetic moment of gadolinium will alter the local magnetic field of blood (ie, change the susceptibility or T2*) relative to surrounding brain parenchyma. In principle, as long as the BBB remains intact, this change in susceptibility will be visualized as signal loss on T2*-weighted images. In the context of BBB disruption, however, the initial signal drop associated with gadolinium passing through the blood vessels within the voxel is followed by an increase in signal intensity as contrast begins to extravasate (ie, a competing T1 effect). Evidence of this secondary signal intensity increase, and/or its extent, forms the basis for exploring DSC-measures as potential surrogate markers of BBB disruption.

One such approach is to measure the relative recirculation of contrast (*rR*).[40] This DSC measure involves separating the intravascular (T2*) and extravascular/recirculation phases (T1) by fitting a theoretical first-pass curve to the ΔR_2^* versus time curve ($\Delta R_2^* = \Delta(1/T2^*)$) and measuring the difference in the areas encompassed by the measured and the fitted curves (**Fig. 5**). Given that contrast extravasation is also associated with BBB disruption in acute ischemic stroke, investigators have begun to evaluate DSC-based surrogates as predictors of hemorrhagic

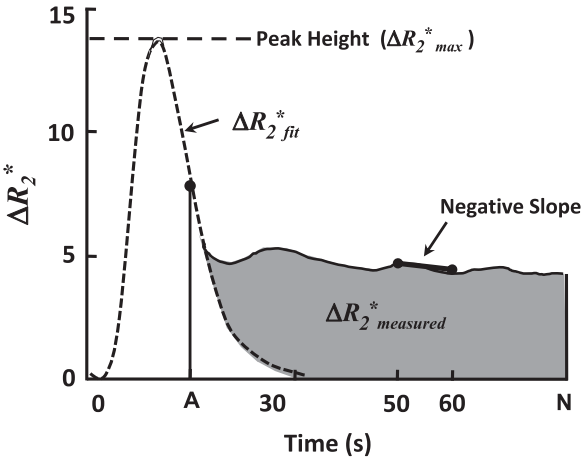

$$\text{Relative recirculation (rR)} = \frac{\sum_{0}^{t}\left[\Delta R2^*_{measured}(t) - \Delta R2^*_{fit}(t)\right]}{\Delta R2^*_{\max}(N - A)}$$

Fig. 5. A ΔR_2* versus time curve (ΔR_2*$_{measured}$), as well as its gamma-variate fit (ΔR_2*$_{fit}$), depicting 3 DSC surrogate measures of BBB permeability: *rR*, Peak Height, and Slope = slope of ΔR_2*$_{measured}$ (t) between 50 and 60 seconds after injection.

complications. Bang and coworkers[42] hypothesized that the change in T2* relaxation rate (ΔR_2*) associated with the last 10 seconds of a 60-second bolus tracking study (negative slope) can predict HT in recanalized acute ischemic stroke patients. In fact, this simple DSC marker appeared to predict future HT with a sensitivity of 83%. More recently, we estimated *rR* in patients with acute ischemic stroke and compared this DSC metric with DCE-MRI estimates of BBB permeability (*KPS*).[43] Preliminary results indicated a strong and significant correlation between *rR* and *KPS*, as well as significant increases in both measures in stroke lesions that proceeded to hemorrhage (compared with those that did not). Taken together, these early findings provide support for our hypothesis that *rR* is related to the extent of BBB leakage and that *rR* may provide a reasonable surrogate for *KPS*.

Although encouraging, it is not presently known whether *rR* is strictly reflective of BBB permeability or rather just microvascular "abnormalities." A more prudent interpretation of these results is that *rR* reflects a superposition of microvascular features, including blood volume, vessel tortuosity and, perhaps, permeability.[40,44] As such, *rR* may be less suitable than *KPS* for the investigation of new therapies and their effects on BBB integrity (eg, where absolute quantification is desirable). Whether or not *rR* will ultimately prove valuable in treatment decision making in acute ischemic stroke remains to be demonstrated.

The next advancement in CT mapping of permeability is likely to be more widespread availability of CT scanners capable of whole-brain CTP coverage. Intrasubject comparison of permeability values obtained with CT versus MRI techniques may help clarify the relative merits of each of these approaches, but serial imaging with closely spaced CT and MRI will be challenging in an acute stroke setting. Perhaps animal model comparison will be useful.

With either CT or MRI, the ability to quickly and accurately predict the likelihood of hemorrhagic transformation may enable a transition from using a fixed therapeutic time window for rtPA administration to treatment decisions based on individual patient risk. This move to individualized risk assessment is certainly a promising area of imaging research in the broadest sense, and permeability imaging may be an early success.

REFERENCES

1. The National Institute of Neurological Disorders and Stroke rt-PA Stroke Study Group. Tissue plasminogen activator for acute ischemic stroke. N Engl J Med 1995;333:1581–7.
2. Hacke W, Kaste M, Bluhmki E, et al. Thrombolysis with alteplase 3 to 4.5 hours after acute ischemic stroke. N Engl J Med 2008;359:1317–29.
3. Hamann GF, Okada Y, del Zoppo GJ. Hemorrhagic transformation and microvascular integrity during

focal cerebral ischemia/reperfusion. J Cereb Blood Flow Metab 1996;16:1373–8.
4. Dijkhuizen RM, Asahi M, Wu O, et al. Rapid breakdown of microvascular barriers and subsequent hemorrhagic transformation after delayed recombinant tissue plasminogen activator treatment in a rat embolic stroke model. Stroke 2002;33:2100–4.
5. Busch E, Kruger K, Fritze K, et al. Blood-brain barrier disturbances after rt-PA treatment of thromboembolic stroke in the rat. Acta Neurochir 1997; 70:206–8.
6. Kelly MA, Shuaib A, Todd KG. Matrix metalloproteinase activation and blood-brain barrier breakdown following thrombolysis. Exp Neurol 2006;200:38–49.
7. Montaner J, Molina CA, Monasterio J, et al. Matrix metalloproteinase-9 pretreatment level predicts intracranial hemorrhagic complications after thrombolysis in human stroke. Circulation 2003;107: 598–603.
8. Yepes M, Sandkvist M, Moore EG, et al. Tissue-type plasminogen activator induces opening of the blood-brain barrier via the LDL receptor-related protein. J Clin Invest 2003;112:1533–40.
9. Weinmann HJ, Laniado M, Mutzel W. Pharmacokinetics of Gd-DTPA/dimeglumine after intravenous injection into healthy volunteers. Physiol Chem Phys Med NMR 1984;16:167–72.
10. Vo KD, Santiago F, Lin W, et al. MR imaging enhancement patterns as predictors of hemorrhagic transformation in acute ischemic stroke. AJNR Am J Neuroradiol 2003;24:674–9.
11. Kim EY, Na DG, Kim SS, et al. Prediction of hemorrhagic transformation in acute ischemic stroke: role of diffusion-weighted imaging and early parenchymal enhancement. AJNR Am J Neuroradiol 2005;26: 1050–5.
12. Kastrup A, Groschel K, Ringer TM, et al. Early disruption of the blood-brain barrier after thrombolytic therapy predicts hemorrhage in patients with acute stroke. Stroke 2008;39:2385–7.
13. Merten CL, Knitelius HO, Assheuer J, et al. MRI of acute cerebral infarcts, increased contrast enhancement with continuous infusion of gadolinium. Neuroradiology 1999;41:242–8.
14. Virapongse C, Mancuso A, Quisling R. Human brain infarcts: Gd-DTPA-enhanced MR imaging. Radiology 1986;161:785–94.
15. Mikulis DJ, Guo G, Wu R, et al. Gadolinium Enhancement Predicts Hemorrhagic Transformation in Acute Ischemic Stroke [abstract: 43]. In: 44th Annual Meeting of the American Society for Neuroradiology. San Diego (CA), May 2006.
16. Latour LL, Kang DW, Ezzeddine MA, et al. Early blood-brain barrier disruption in human focal brain ischemia. Ann Neurol 2004;56:468–77.
17. Wang X, Tsuji K, Lee SR, et al. Mechanisms of hemorrhagic transformation after tissue plasminogen activator reperfusion therapy for ischemic stroke. Stroke 2004;35:2726–30.
18. Kassner A, Roberts TP. Beyond perfusion: cerebral vascular reactivity and assessment of microvascular permeability. Top Magn Reson Imaging 2004;15: 58–65.
19. Cheng HL. Investigation and optimization of parameter accuracy in dynamic contrast-enhanced MRI. J Magn Reson Imaging 2008;28:736–43.
20. Kassner A, Roberts T, Taylor K, et al. Prediction of hemorrhage in acute ischemic stroke using permeability MR imaging. AJNR Am J Neuroradiol 2005; 26:2213–7.
21. Roberts TP. Physiologic measurements by contrast-enhanced MR imaging: expectations and limitations. J Magn Reson Imaging 1997;7:82–90.
22. Pruessmann KP, Weiger M, Scheidegger MB, et al. SENSE: sensitivity encoding for fast MRI. Magn Reson Med 1999;42:952–62.
23. Donahue KM, Weisskoff RM, Burstein D. Water diffusion and exchange as they influence contrast enhancement. J Magn Reson Imaging 1997;7: 102–10.
24. Larsson HB, Stubgaard M, Frederiksen JL, et al. Quantitation of blood-brain barrier defect by magnetic resonance imaging and gadolinium-DTPA in patients with multiple sclerosis and brain tumors. Magn Reson Med 1990;16:117–31.
25. Brix G, Semmler W, Port R, et al. Pharmacokinetic parameters in CNS Gd-DTPA enhanced MR imaging. J Comput Assist Tomogr 1991;15:621–8.
26. Tofts PS, Kermode AG. Measurement of the blood-brain barrier permeability and leakage space using dynamic MR imaging: 1. Fundamental concepts. Magn Reson Med 1991;17:357–67.
27. Patlak CS, Blasberg RG, Fenstermacher JD. Graphical evaluation of blood-to-brain transfer constants from multiple-time uptake data. J Cereb Blood Flow Metab 1983;3:1–7.
28. Patlak CS, Blasberg RG. Graphical evaluation of blood-to-brain transfer constants from multiple-time uptake data. Generalizations. J Cereb Blood Flow Metab 1985;5:584–90.
29. Tofts PS, Brix G, Buckley DL, et al. Estimating kinetic parameters from dynamic contrast-enhanced T(1)-weighted MRI of a diffusable tracer: standardized quantities and symbols. J Magn Reson Imaging 1999;10:223–32.
30. Roberts HC, Roberts TP, Brasch RC, et al. Quantitative measurement of microvascular permeability in human brain tumors achieved using dynamic contrast-enhanced MR imaging: correlation with histologic grade. AJNR Am J Neuroradiol 2000;21: 891–9.
31. Ewing JR, Knight RA, Nagaraja TN, et al. Patlak plots of Gd-DTPA MRI data yield blood-brain transfer constants concordant with those of 14C-sucrose

in areas of blood-brain opening. Magn Reson Med 2003;50:283–92.
32. Knight RA, Barker PB, Fagan SC, et al. Prediction of impending hemorrhagic transformation in ischemic stroke using magnetic resonance imaging in rats. Stroke 1998;29:144–51.
33. Kassner A, Liu F, Matta S, et al. Quantitative dynamic contrast-enhanced MRI: a potential tool for guiding treatment decisions in acute ischemic stroke. In: Joint Annual Meeting ISMRM-ESMRMB. Berlin (Germany), May 2007. p. 499.
34. Ding G, Jiang Q, Li L, et al. Detection of BBB disruption and hemorrhage by Gd-DTPA enhanced MRI after embolic stroke in rat. Brain Res 2006;1114: 195–203.
35. Vidarsson L, Thornhill RE, Liu F, et al. Quantitative permeability MRI in acute ischemic stroke: how long do we need to scan? Magn Reson Imaging 2009;27(9):1216–22.
36. Dankbaar JW, Hom J, Schneider T, et al. Dynamic perfusion CT assessment of the blood-brain barrier permeability: first pass versus delayed acquisition. AJNR Am J Neuroradiol 2008;29:1671–6.
37. Lin K, Kazmi KS, Law M, et al. Measuring elevated microvascular permeability and predicting hemorrhagic transformation in acute ischemic stroke using first-pass dynamic perfusion CT imaging. AJNR Am J Neuroradiol 2007;28:1292–8.
38. Hom J, Dankbaar JW, Schneider T, et al. Optimal duration of acquisition for dynamic perfusion CT assessment of blood-brain barrier permeability using the Patlak model. AJNR Am J Neuroradiol 2009;30:1366–70.
39. Aviv RI, d'Esterre CD, Murphy BD, et al. Hemorrhagic transformation of ischemic stroke: prediction with CT perfusion. Radiology 2009;250:867–77.
40. Kassner A, Annesley DJ, Zhu XP, et al. Abnormalities of the contrast re-circulation phase in cerebral tumors demonstrated using dynamic susceptibility contrast-enhanced imaging: a possible marker of vascular tortuosity. J Magn Reson Imaging 2000; 11:103–13.
41. Lupo JM, Cha S, Chang SM, et al. Dynamic susceptibility-weighted perfusion imaging of high-grade gliomas: characterization of spatial heterogeneity. AJNR Am J Neuroradiol 2005;26: 1446–54.
42. Bang OY, Buck BH, Saver JL, et al. Prediction of hemorrhagic transformation after recanalization therapy using T2*-permeability magnetic resonance imaging. Ann Neurol 2007;62:170–6.
43. Wu SP, Vidarsson L, Winter J, et al. Estimates of relative contrast recirculation obtained from perfusion MRI: a potential tool for guiding treatment decision in acute ischemic stroke. In: 16th Scientific Meeting and Exhibition of the ISMRM. Toronto (ON), May 2008. p. 307.
44. Jackson A, Kassner A, Annesley-Williams D, et al. Abnormalities in the recirculation phase of contrast agent bolus passage in cerebral gliomas: comparison with relative blood volume and tumor grade. AJNR Am J Neuroradiol 2002;23:7–14.